Reprint
8th Int. Symp. Field Measurements in GeoMechanics, Berlin, Germany (2011): CD - 18 p.

Long term Measurement and Analysis of a Deep-Seated Mass Movement

Martin Müller[1], Fritz K. Brunner[1], Erich Lang[2]

[1]Graz University of Technology, Department of Engineering Geodesy and Measurement Systems, Austria

[2]Federal Research and Training Centre for Forests, Natural Hazards and Landscape (BFW), Austria

1 Introduction

The Gradenbach deep-seated mass movement is located at the intersection of Gradenbach river with the upper Möll valley in Carinthia (Austria). Key figures are summarized in Table 1, Figure 1 shows the landslide area. The main potential hazard of this landslide is the blockage of the Gradenbach river. This can lead to serious damage, as soon as the accumulated material would burst through and devastates the settlement of Putschall in the nearby Möll valley. This was the case already in 1965 and 1966 having also resulted in the development and implementation of a geodetic, geotechnical and hydrological monitoring.

Table 1: Key figures of the Gradenbach deep-seated mass movement

Slant length	1800 m
Width	800 m
Average thickness	80 m
Elevation difference	1000 m
Average inclination	30 °
Moving volume	$115 \cdot 10^6$ m^3
Velocity	60 – 600 mm/a

Since 1999 the Department of Engineering Geodesy and Measurement Systems operates four GPS monitoring stations in the landslide area. They consist of low-cost single frequency receivers with geodetic choke ring antennas on tripods, belaid with cables. Before 2009 they were set up in two campaigns per year, recording a 48 h session each time. Since 2009 stations MA (for location

see Figure 1) and R2 are recording continuously to data loggers, which are downloaded twice a year. Data processing is done for 6 sessions per day. In 2010 MC, R1 and R2 were upgraded with GPRS modems, transmitting GPS raw data to the office in Graz, where they are processed automatically. The results are accessible to Carinthia's governmental geologist on an FTP-server. We use the software BERNESE 6.0 for GPS data processing with R2 serving as reference station. Since 2010 we have not calculated atmospheric biases in BERNESE, but have applied corrections, derived from the coordinate biases of a second reference station (R1), as described by Schön et al. (2005) and Schön (2007).

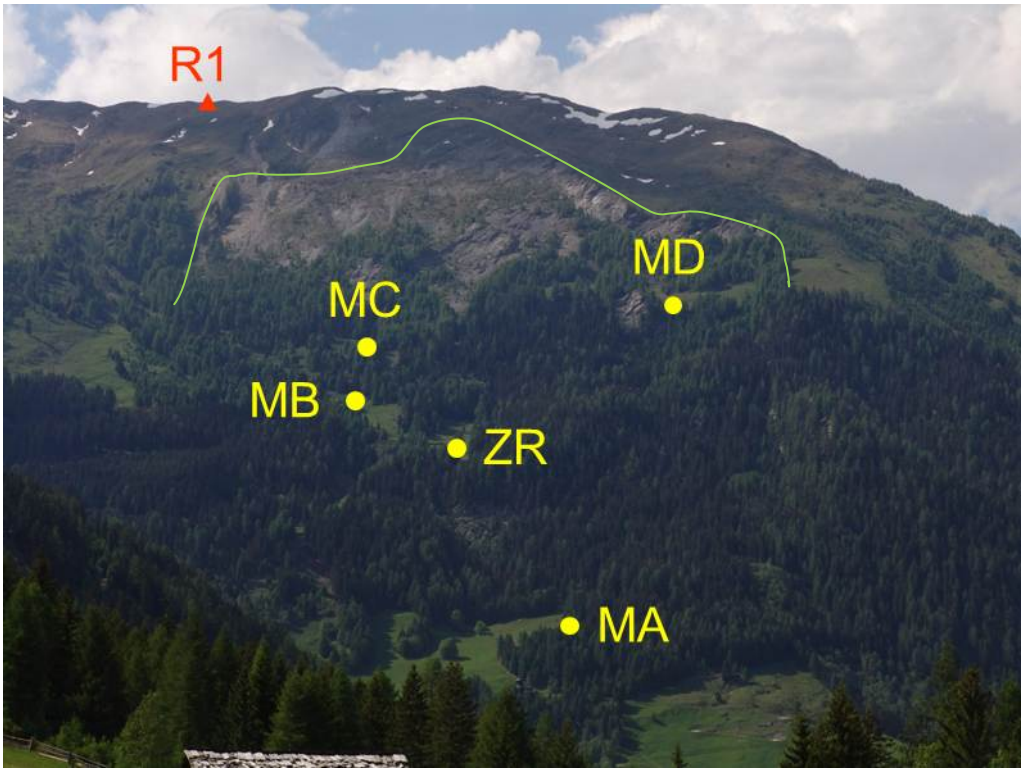

Figure 1: View of Gradenbach deep-seated mass movement. Yellow: positions of GPS monitoring points. Point ZR is not occupied regularly. Red: one of two GPS reference stations on stable ground. The other one (R2) is close to the position of the photographer. Green line: main scarp of landslide

Figure 2 shows the extent of the landslide area and point velocities from an aerial view. Interestingly, two points (R1, R3) are moving very slowly but parallel to the landslide motion, though they are far outside the actual landslide area: R3 (11 mm/a) and R1 (1.2 mm/a), both velocities 3D. Unfortunately, R1

serves as second GPS reference station. It is possible, however, to describe its movement as a linear function of time.

This paper mainly will be concerned with the analysis of coordinate time series of GPS monitoring points MA, MB, MC and MD between 1999 and 2010, using one reference station (R2) and estimating atmospheric effects in BERNESE. Additional data will be used from a wire extensometer close to surveying point FL (Figure 2). Its two anchor points are located at the toe of the landslide and the counter slope of Gradenbach river. Assuming that the counter slope is stable, then the movement of the toe of the landslide is measured. Recent terrestrial survey revealed, however, that the counter slope was moving slowly (about 40 mm/a), which increased the extensometer velocities.

2 Precision of GPS coordinates

By precision of GPS coordinates we understand the empirical std (standard deviation) of sessions of 24 h. It was calculated from two datasets, after eliminating 3 % of data as outliers:

- 370 sessions of R1 between 2009 06 14 and 2009 10 12, as well as between 2010 06 05 and 2011 04 17,
- 309 sessions of MA between 2009 06 01 and 2010 07 31. As MA is moving, we calculated the std of unit weight of a polynomial fit.

The resulting std's are within one mm, the averaged std's amount to 2 mm horizontally and 5 mm vertically. Using a second reference station would reduce the vertical std. However, we calculated the here presented time series using only one reference station, because until 2008 the second one was not occupied during all sessions.

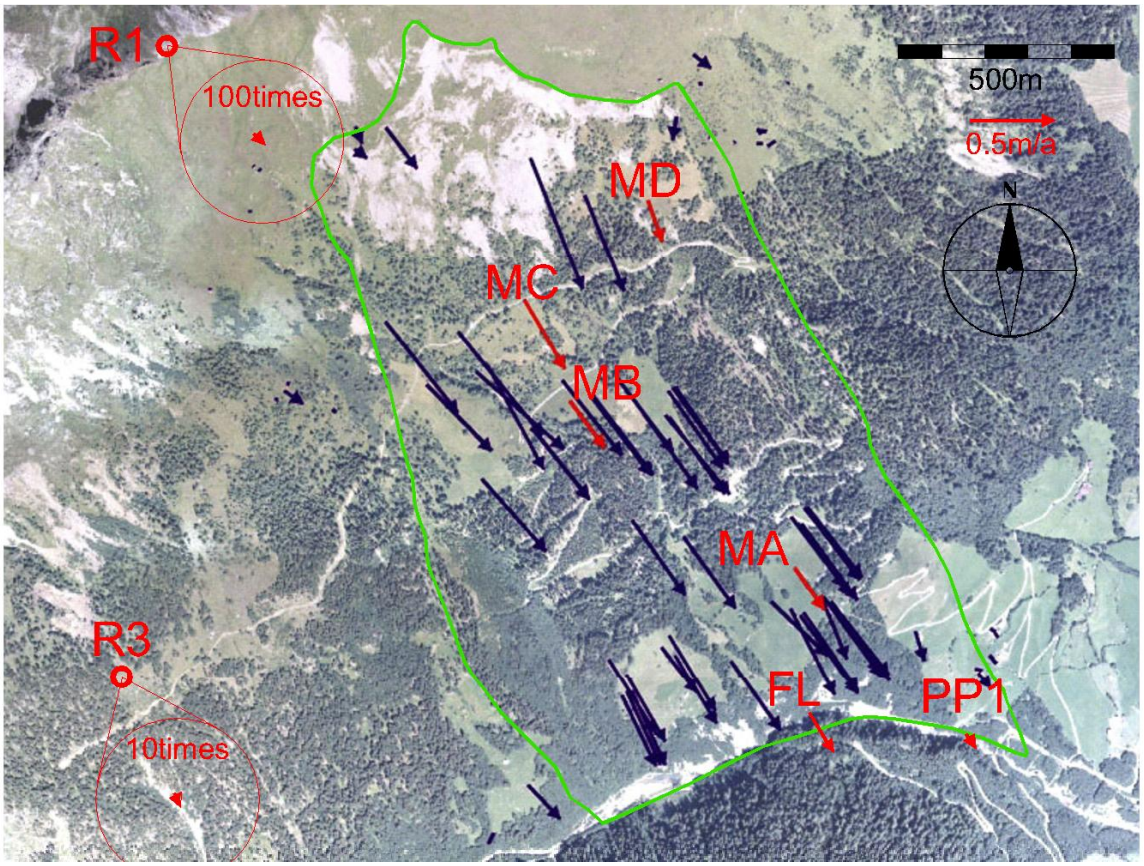

Figure 2: Aerial view with the plotted horizontal movements. Green border: outcrop of base of landslide according to seismic study (Brückl and Brückl 2006). Blue arrows: velocities from photogrammetry (Brückl et al. 2006). Red arrows: velocities from GPS- and terrestrial surveys between 1999 and 2003, FL and PP1 from terrestrial survey, all other points from GPS. R1 and R3 are plotted with zooms showing the very small motions

3 Local coordinate systems of monitoring points

The WGS84 coordinates, computed directly by GPS data processing, are transformed into Gauss-Krüger coordinates and ellipsoidal heights, called ‘state coordinate system’ (see Figure 3). Differences to the actual Austrian state coordinates are less then 20 cm horizontally and amount to 2 m in elevation with no rotation.

It is disadvantageous to use these coordinates for a study of time series: In very good approximation, the movement of a monitoring point is a straight line, called main component of movement, which is not parallel to any of the three

coordinate axes. Thus, time series of any coordinate component are dominated by the main velocity component, and therefore, small deviations become hardly visible. An easy way to separate them from the main velocity component is the use of local coordinate systems, different for each monitoring point. The directions of the local coordinate axes result from a principal component analysis of the state coordinate time series, i.e. they are the eigenvectors of the covariance matrix of state coordinates. Components of local coordinates are the projections of the point positions onto the eigenvectors. As these projections must be uncorrelated, the main component of movement must be parallel to one of the local coordinate axes.

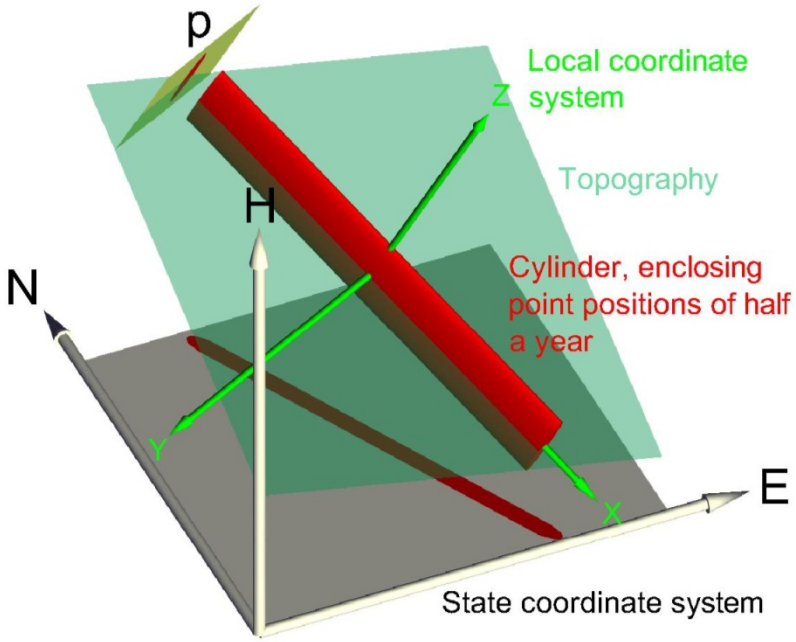

Figure 3: Local coordinate system of a monitoring point (green) related to the state coordinate system (white). The plane p is parallel to the YZ-plane of local coordinates and outlines the top view of the red cylinder

The components can be arranged according to their std, where the largest std belongs to the main component of movement. Obviously, it is parallel to the fall line through the monitoring point. The remaining two components show much smaller std's and decompose the lateral deviations into an approximately horizontal component, and a third one, approximately normal to the slope. The main component defines the X-axis of the local coordinate system. The horizontal deviation defines the Y-axis. The deviation normal to the slope is the

Z-axis. The origin of the local coordinate system is assumed to be the mean position between 1999 and 2010.

It is possible to enclose the movement of a monitoring point in an elliptical cylinder, whose long axis coincides with the local X-axis and whose half axes of the ellipse coincide with the Y- and Z-axis (Figure 3). The length of this cylinder depends on the duration of the observation period, because the main component of movement is a monotonically nondecreasing function of time, whose first derivative is the velocity. The lengths of half axes of the ellipse don't change with time, because the lateral deviations are periodical functions of time. Their amplitudes define the lengths of the half axes: roughly 10 mm normal to the slope and 3 mm horizontal. The period is equal for both deviations, but changes with time. Duration of the most recent period is 8 years.

This method of separating the landslide motion into the main component of movement and lateral deviations by the introduction of local coordinates shows one problem: adding data to the time series results in a change of the state coordinate covariance matrix, a rotation of its eigenvectors and thus in a rotation of local coordinate axes. To assess the magnitude of this effect, we set up a first order model of movement:

- Main component is a straight line of progress *s*
- Deviations *d* normal to the slope are a function of the progress *s* of main component:

$$d(s) = A\sin(\omega s + \delta),\ A = 0.01,\ \omega = \frac{2\pi}{1.8},\ \delta = \frac{\pi}{2} \tag{1}$$

  Lengths in meters

- Horizontal deviations are negligible

The chosen parameters create a simple 2D-model of a typical monitoring point, valid for the past 10 years, origin of main component in 2000. Calculating the eigenvectors reveals: the angle between eigenvectors and predefined coordinate axes converges to zero, and remains below 1 gon after one period.

As the time span of observations is longer than one period of deviations, the orientation of the local coordinate systems will not change significantly.

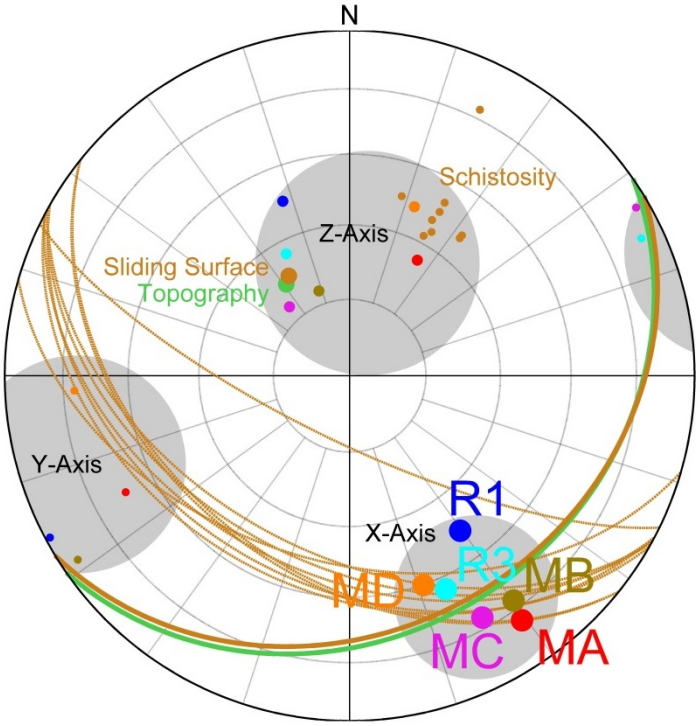

Figure 4: Equal area projection, showing intersection of lines and planes with the lower hemisphere as points and great circles. Coloured dots: local coordinate axes of monitoring points. Grey disks mark general orientations of local coordinate systems. Green: topography (point of intersection of normal and great circle of intersection of plane), Brown: schistosity or basal plane of landslide (bold)

Figure 4 indicates:

- Basal plane of landslide (Brückl and Brückl, 2006) and mean plane of topography are parallel.
- Intersection of schistosity with basal plane and topography is parallel to the fall line. This disjoints the slope into bars, parallel to the fall line, thus facilitating landslide formation.

X-axes of local coordinate systems, i.e. direction of main components of movement, coincide with intersection of schistosity with basal plane and

topography. Z-Axes are partially normal to basal plane and partially normal to the planes of schistosity.

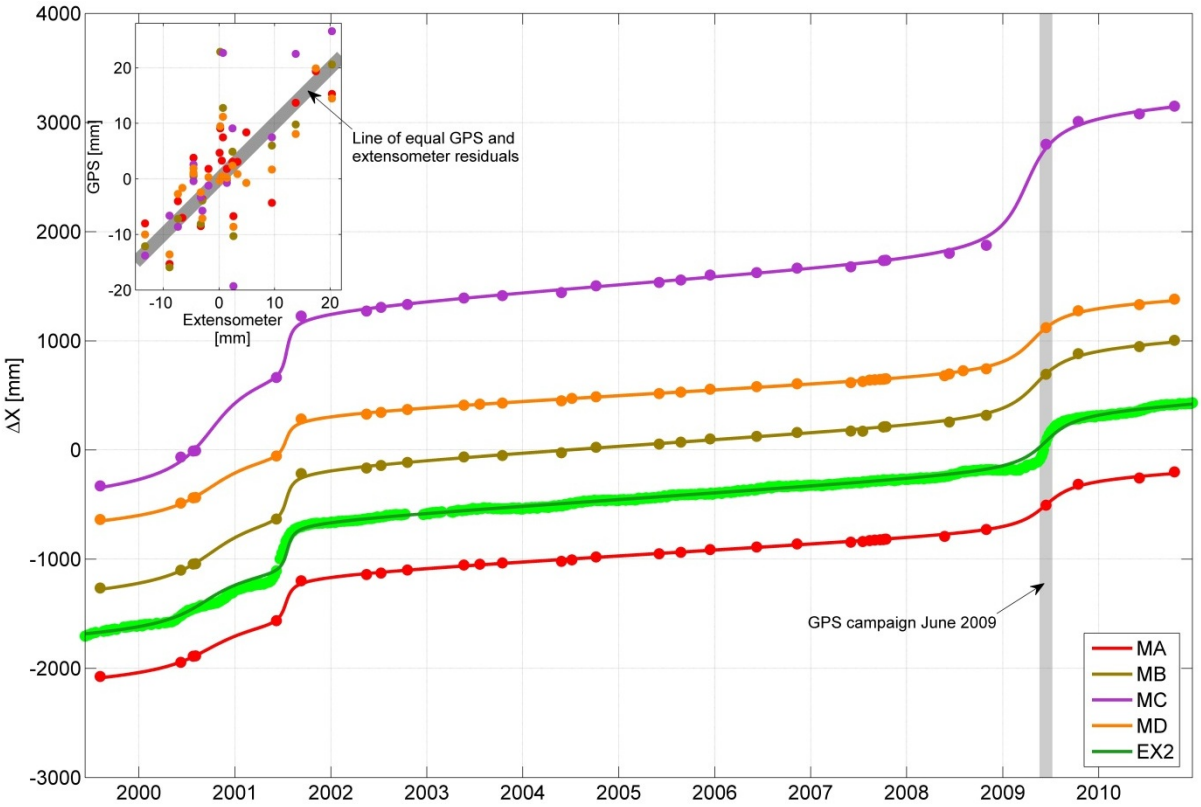

Figure 5: Regression lines of main components of movement derived from GPS- and extensometer time series. EX2: extensometer. Time series are shifted parallel to the abscissa by an arbitrary amount for clarity. Inset: regression residuals of extensometer versus GPS data

4 Main component of movement

4.1 Raw time series

Figure 5 shows the time series of the main components of all GPS monitoring stations since 1999, original observations (dots) as well as regression functions (lines). There were two short periods of high velocities (2001 and 2009), separated by a rather long period of slow velocity. Such successions of high and slow velocities are frequent phenomena of landslides (Brückl, personal communication). The reasons for the landslide accelerations are not yet exactly known. However, there is an obvious connection with high amount of precipitation during the preceding months.

In addition to the GPS time series, Figure 5 includes extensometer readings from the toe of landslide (Chapter 1). The extensometer consists of two steel wires at an angle of 45°, with one wire (EX2) being parallel to the main component of slope movement. Figure 5 highlights two facts, which are relevant for further discussions about the main component:

- We can see from the GPS campaign of June 2009: different stations are at different development stages of acceleration and deceleration. It should be noted that the GPS campaign happened at the same time for all stations. The time shift of development stages is greatest between MA and MC: while deceleration nearly had finished at MC, MA just experienced its highest velocity.
- Regression residuals from the period of slow movement correlate well between all stations in general, and between GPS and extensometer in particular (inset in Figure 5).

Until 2009, the GPS coordinate time series has consisted of data collected at about half year intervals (see Chapter 1), which is too coarse to find out more details about the time shifts, suggested in Figure 5. On the other hand, extensometer observations are available every week. The good correlation between GPS- and extensometer residuals suggests an estimation of GPS results at weekly intervals from extensometer data. This time resolution is fine enough for a detailed study of the time shifts.

4.2 Estimation of epochs at weekly intervals

We estimated for the GPS time series epochs at the times of the extensometer observations, using the following sequence of calculations (slightly simplified):

- Fitting of regression functions to the main components of movement for extensometer and GPS time series:

$$\Delta X(t) = d + ct + \sum_i A_i \arctan(\omega_i t + \delta_i) \qquad (2)$$

ΔX	Main component of movement,
t	Time,
$d+ct$	Linear part of regression function,

A_i, ω_i, δ_i Coefficients, scaling and shifting arctangent functions, modelling the steps in the time series.

For the regression analysis of extensometer data only those epochs were used for which GPS data are available.

- In the second step, the regression function of the extensometer time series was synchronised with the GPS time series, yielding one synchronous extensometer time series for each GPS time series.
- Estimation of regression residuals for the GPS time series at weekly epochs using Cokriging. Residuals of original GPS epochs and of the entire set of synchronised extensometer epochs were used as input for Cokriging. The solution of the Cokriging system is:

$$\begin{pmatrix} \lambda_P(t) \\ \lambda_X(t) \\ \mu \\ \nu \end{pmatrix} = \mathbf{K}^{-1}\mathbf{k}(t) = \begin{pmatrix} \Sigma_{PP} & \Sigma_{PX} & \mathbf{1} & \mathbf{0} \\ \Sigma_{PX}^T & \Sigma_{XX} & \mathbf{0} & \mathbf{1} \\ \mathbf{1}^T & \mathbf{0}^T & 0 & 0 \\ \mathbf{0}^T & \mathbf{1}^T & 0 & 0 \end{pmatrix}^{-1} \begin{pmatrix} \sigma_{P\hat{P}}(t) \\ \sigma_{X\hat{P}}(t) \\ 1 \\ 0 \end{pmatrix} \tag{3}$$

λ_P Vector of coefficients to the known GPS epochs contributing to the estimation,

λ_X Vector of coefficients to the known extensometer epochs contributing to the estimation,

μ, ν Lagrange multipliers,

t Epoch of estimation,

Σ_{PP} Covariance matrix of known GPS epochs,

Σ_{PX} Cross-covariance matrix of known GPS and extensometer epochs,

Σ_{XX} Covariance matrix of known extensometer epochs,

$\sigma_{P\hat{P}}$ Vector of covariances of estimated and known GPS epochs,

$\sigma_{X\hat{P}}$ Vector of cross-covariances of estimated GPS and known extensometer epochs.

As the formula indicates, the linear coefficients λ_P and λ_X forming the estimation are functions of the estimation epoch t. As t does not occur in the inverse of the Krigematrix **K**, it is easily possible to analytically calculate the time derivatives of the estimation, yielding velocity and acceleration.

- Final estimation is the sum of regression function and estimated residuals.

Figure 5 shows the fit of regression functions which already model the time series quite well. Largest residuals remain for epochs near the beginning and the end of the high velocity periods (end of 2001 and 2009). After the Cokriging of residuals, those differences disappear (Figure 6), the periods of high velocity become shorter and the accelerations larger.

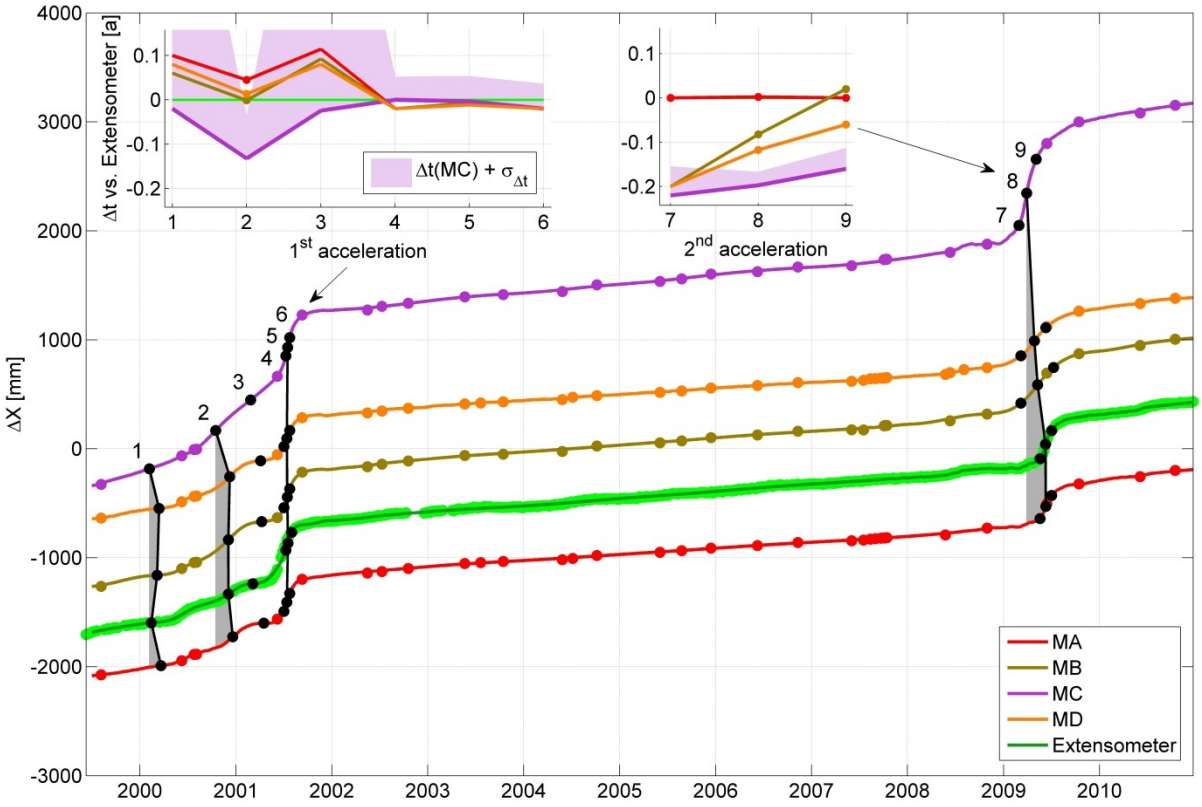

Figure 6: Estimation of GPS time series at weekly epochs (coloured lines). Coloured dots: observation campaigns. Black dots: distinctive points in the course of movement, identifiable in all time series, allowing calculation of time delays between different time series. Grey shaded areas help estimate the time delays of distinctive points in different time series. Small insets: time delays of distinctive points, relative to extensometer results. Magenta shaded areas: mean std of delays between MC and other time series

Continuous monitoring of station MA since summer 2009 has allowed a comparison of the observed deceleration with the estimated values. During the deceleration period, coincidence is very good (less than 2 cm). During the

successive period of slow movement, continuous GPS monitoring has revealed a short acceleration period, too short for the resolution of extensometer observations. Thus, it is not visible in the estimation and causes differences up to 4 cm between estimation and continuous monitoring.

4.3 Chronology of acceleration and deceleration of main component of movement

Using velocity- and acceleration time series, calculated as described previously together with Cokriging, it is possible to define distinctive points in the course of movement. They are identifiable in all time series and allow calculation of the time shifts between different monitoring points, introduced above (numbers refer to Figure 6):

- 4,7: maximal acceleration,
- 2,5,8: maximal velocity,
- 6,9: maximal deceleration,
- 1: start of acceleration (difficult to determine accurately).

As the shaded areas in Figure 6 indicate, the delay between the motion states MC (earlier) and MA (later), as assumed above, is verified. Including the remaining of monitoring stations, delays referred to extensometer are less than three months (they are better visible in the inset). During the first period of high velocity (2000-2002) the delays decrease and finally disappear. On the other hand there is a good correlation between minor deviations from the regression functions during the long period of slow movement (2002-2009), without applying any time shift (inset in Figure 5). This means, acceleration of movement starts asynchronously, but successive deceleration ends up again in synchronous, slow movement. Figure 7 displays time delay between all monitoring stations in a map together with contour lines of landslide thickness. The late onset of the acceleration of MA seems to be caused by an underground ridge, protecting the surrounding of MA from the mass of the landslide pushing down from the higher parts of the slope. Generally, there is an indication of a trend, that central or higher parts of the landslide start to accelerate earlier than the lateral or lower ones.

The two periods of acceleration during the time of our monitoring since 1999 did not cause considerable damages (only the rockfall activity increased considerably in the upper part of the slope during the last years). However, any acceleration has the potential to mount up and cause dangerous velocities, resulting in the requirement to monitor the landslide and setup alerting procedures. Due to the above conclusions about acceleration chronology, MC is a good choice for online processing (see Chapter 1), as it is the highest monitoring point in the central part of the landslide. It's time advance will most likely allow timely alert.

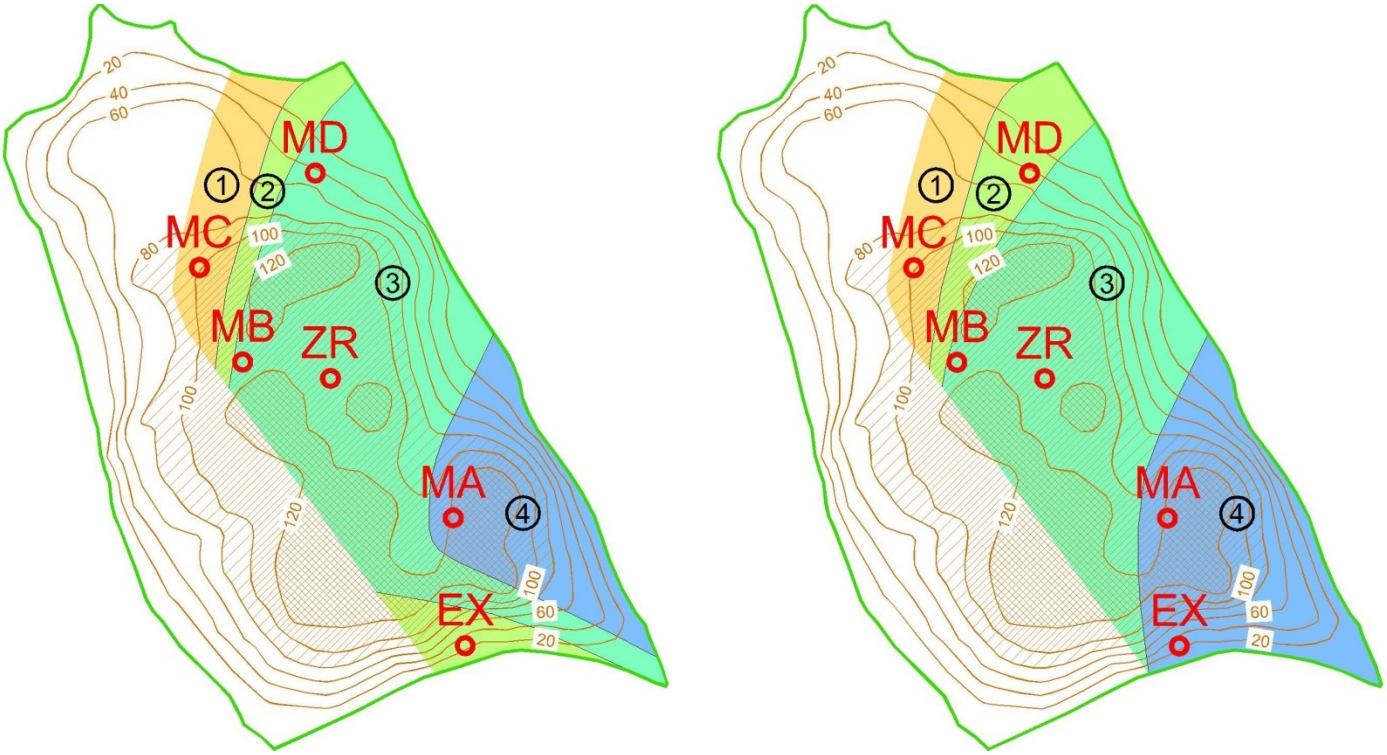

Figure 7: Order of onset of acceleration in a map of the landslide. Left: high velocity period 2000-2002, right: 2008-2009. ZR was not input to calculations, EX: extensometer. Contour lines show the depth (m) of the basal surface according to Brückl and Brückl (2006)

5 Lateral deviations from the main component of movement

Figure 8 is the projection of trajectories of all GPS monitoring points onto the YZ-plane of their local coordinate systems. The observer looks from above in direction of the main component of movement. The surprising result is that the

projected points are orbiting the main component of movement. The radius of orbit is twice as long parallel to the Z-axis than the radius of orbit parallel to the Y-axis. During periods of slow movement points are below and during periods of high velocity they are above the main component of movement (coloured background markers in Figure 8). It is worth mentioning that they are usually not situated directly on the line of the main component of movement itself. The time between the two epochs of high velocity is also the period of lateral deviations (8 years), already mentioned in Chapter 3. Due to the link between velocity and deviations, just described above, the duration of this period will change with time: Amount of precipitation (rainfall, snowmelt) triggers velocity, which governs lateral deviations in turn. This means, precipitation causes deviations, which is not a periodical phenomenon.

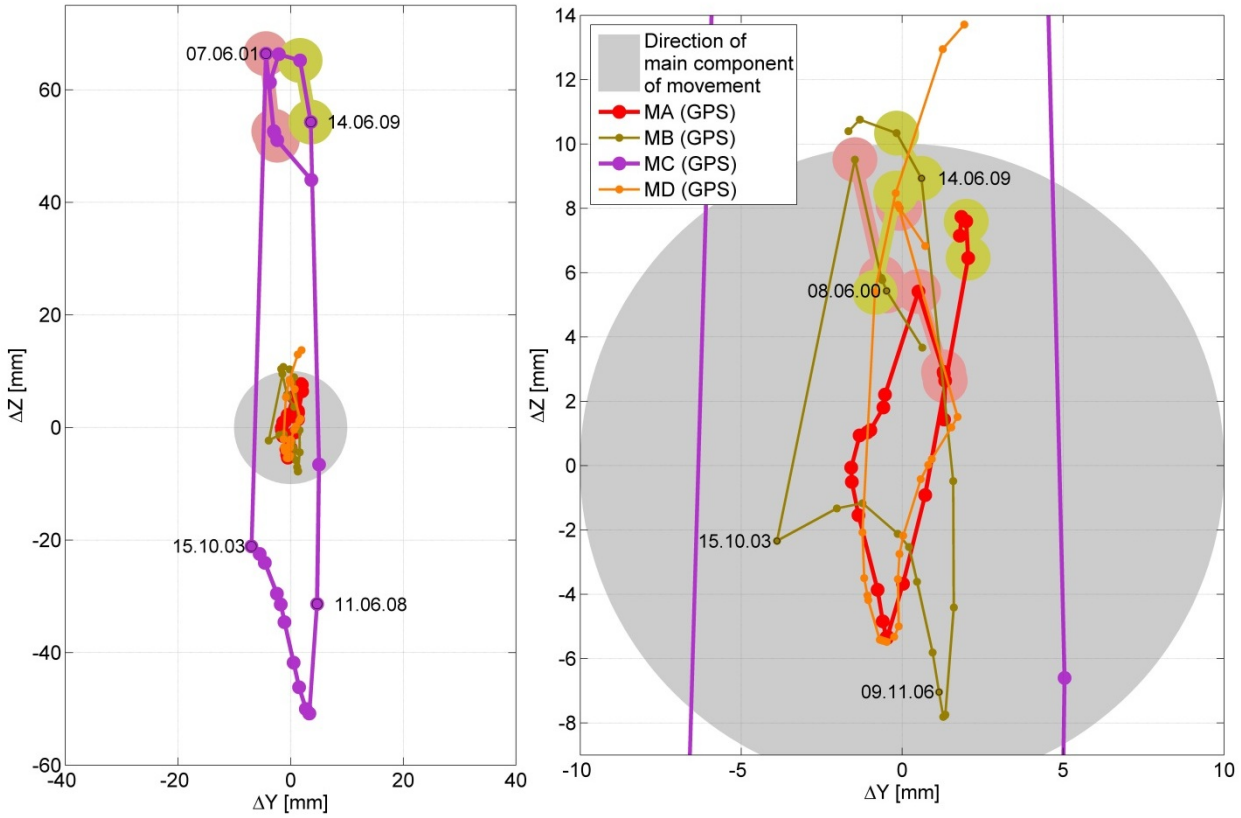

Figure 8: Projection of movement onto the YZ-plane of local coordinate systems, main component is the center of the grey disk. Coloured background markers: periods of high velocity. Smoothed with a filterlength of 1200 days. Right plot is an enlargement of the left plot

Scaling of local coordinates with their inverse std's shortens the main components of movement heavily. Thus they don't hide the deviations in a 3D plot like Figure 9 and the interaction of main component and lateral deviations becomes clearly visible.

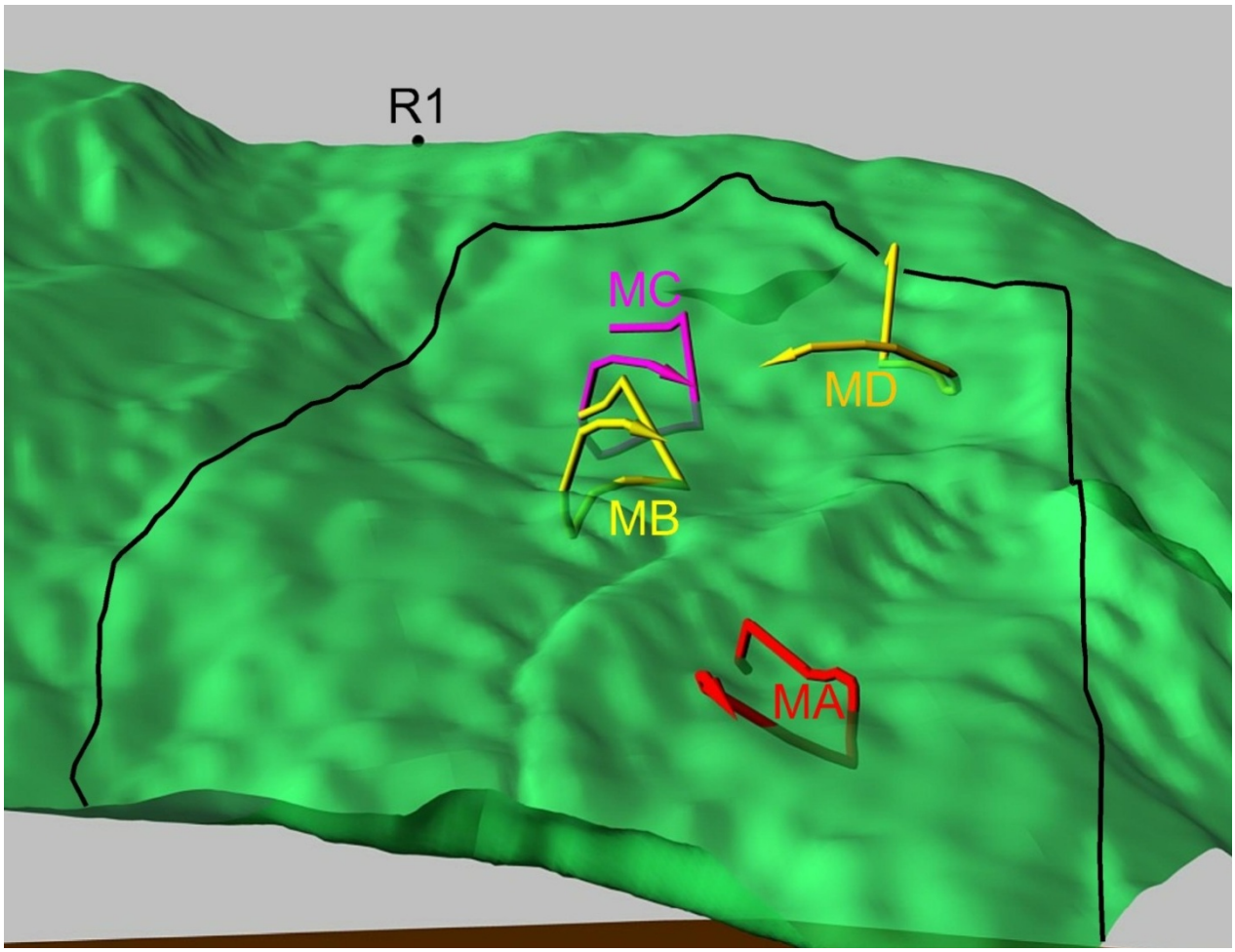

Figure 9: Movement of monitoring points since 1999, after scaling local coordinates with their inverse std's. The paths are heavily distorted, but their spiral shaped route becomes visible. Black line: outcrop of base of landslide according to a seismic study (Brückl and Brückl 2006)

The small size of lateral deviations raises the question, if precision of coordinates derived from GPS observations is sufficiently accurate. Actually, apart from MC, horizontal deviations are no more than the empirical precision (Chapter 2). However, conclusions made above were based on smoothed data, using a filter length of 1200 days and a Gauss function for weighting. It is very likely that data are not correlated, because they originate from campaigns at

half-years intervals. Under the assumption of absent correlations, std's of smoothed data are reduced by a factor of 0.4 and thus become considerably less than the deviations.

A statistical test, applicable to this situation, proceeds from the assumption of pure random deviations. In this case the ratio between mean squared deviation and empirical coordinate variance must follow a Fisher distribution. The tests were done with horizontal deviations and deviations normal to slope separately, as well as with all deviations at once. The test result is negative in all cases, for all monitoring points at a 5 % error risk. This means, deviations are not random, the described paths are real.

The causes of the systematic deviations from the straight main component of movement must be investigated for horizontal deviations and deviations normal to slope separately. The reason for deviations normal to the slope during epochs of high velocity is most likely a transverse dilatation due to the material moving into the monitoring points from above. The reasons for the horizontal deviations are still unknown. Possibly, there is a minor movement along schistosity, whose dip runs transversely to the main component of movement (Figure 4).

6 Summary

We made a detailed analysis of the kinematics of the Gradenbach landslide. For this purpose, it was necessary to decompose the movement into one main component, being downhill, and two lateral deviations which are found to be periodical. Usually, the main component is slow but it accelerates and decelerates at irregular intervals. Potentially, some of the accelerations can lead to a blockage of the Gradenbach river and result in dangerous mud and debris flows. The periods of the lateral deviations are coupled with the accelerations of the main component of movement.

Due to a good correlation between main component of movement, monitored by several GPS stations at approximately half-year intervals, and movements determined by wire extensometer readings at weekly intervals, it was possible

to estimate the main component of movements of the GPS stations also at weekly intervals, using Cokriging. This helped, realizing time delays between the accelerations at the GPS stations, how accelerations propagate across the slope and, most notably, where they start. With this knowledge it was possible to identify the monitoring station, where the acceleration occurs first, gaining a time advance of nearly three months for early warnings.

This paper is based on the time series produced over 13 years of continuous monitoring of a landslide, which is an unusual long time span in this context. However, none of the presented results would have been possible using a shorter time span of data:

- Periods of acceleration and deceleration were separated by 8 years. However, it was necessary monitoring each of them from the very beginning, to study their chronology. Moreover, it needed at least the monitoring of two such periods to separate random features from systematic ones. Thus, monitoring of long time periods of slow movements is required.
- Moreover, the period of lateral deviations is coupled with the time span between accelerations and amounts also to 8 years

The mechanisms of the horizontal component of lateral deviations are still being investigated.

7 Acknowledgements

The extensometer is operated by the Federal Research and Training Centre for Forests, Natural Hazards and Landscape (BFW). The studies presented in this paper were funded by the Austrian Academy of Sciences as part of the project ‚International Strategy for Disaster Reduction'. We thank Prof. Dr. E. Brückl for his long term cooperation.

References

E. Brückl; F.K. Brunner; K. Kraus; Kinematics of a deep-seated landslide derived from photogrammetric, GPS and geophysical data, *Engineering Geology, 88, p. 149-159, 2006*.

E. Brückl; J. Brückl; Geophysical models of the Lesachriegel and Gradenbach deap-seated mass movements (Schober range, Austria), *Engineering Geology, 83, p. 254-272, 2006.*

S. Schön; A. Wieser; K. Macheiner; Accurate Tropospheric Correction for Local GPS Monitoring Networks With Large Height Differences, *ION GNSS 18th International Technical Meeting of the Satellite Division, September 13-16 2005 in Long Beach, CA, p. 250-260, 2005.*

S. Schön; Affine distortion of small GPS networks with large height differences, *GPS Solutions 11, p. 107-117, 2007.*

Authors

Mag. DI. Martin Müller martin.mueller@tugraz.at
Univ.-Prof. DI. Dr. Fritz K. Brunner fritz.brunner@tugraz.at

Engineering Geodesy and Measurement Systems
Graz University of Technolgy
Steyrergasse 30/II, A-8010 Graz http://www.igms.TUGraz.at

DI. Erich Lang erich.lang@bfw.gv.at

Department of Natural Hazards and Alpine Timberline
Federal Research and Training Centre for Forests, Natural Hazards and Landscape
Hauptstrasse 7, A-1140 Wien http://bfw.ac.at